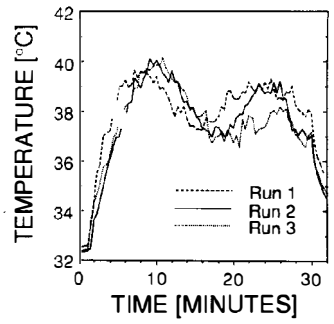

Fig. 7. Repeatability of temperature response for three separate tests with the temperature controlled flow rate parameter at a gain of four, a basal flow rate of 8 mL/min, and a response delay of 4 min.

of random measurement errors. Thus, the temperature perceived by the flow control algorithm is slightly different from the temperature drawn in Fig. 6. Second, the previously described flow rate setting algorithm had a maximum error band of ± 1.5 mL/min in this flow range.

To illustrate the repeatability of this system, the results from a set of three experiments which were preformed with these temperature control parameters are shown in Fig. 7. The close grouping of the temperature profiles indicated that the phantom can yield repeatable results. Finally, one should be careful when attempting to extrapolate the *absolute quantitative* results to real tumors because of the previously mentioned differences in absorbtivity and perfusion patterns between this dynamic phantom and tumors.

Summary

The dynamic phantom presented in this work is a flexible system which can produce repeatable results. It has been successfully used to vary flow rates either according to preprogrammed changes (e.g., step and ramp changes), or in a dynamic pattern controlled by a measured variable (e.g., temperature controlled flow rates). The capabilities of this system imparted by it's computer based nature could lead to automated testing, and this could greatly speed investigations of hyperthermia controllers. Results from preliminary tests of a PID (proportional-integral-derivative) controller are given in Zaerr [15]. We have used the flexibility of the computer algorithm controlled flow to reproduce previously observed *in vivo* temperatures oscillations [11] in this *in vitro* preparation [20].

References

[1] C. K. Chou, "Phantom for electromagnetic heating studies," In *Physics and Technology of Hyperthermia*, S. B. Field and C. Franconi Dordrecht: Nijoff, 1987, pp. 294-318.

[2] T. C. Cetas, "Physical models (phantoms) in thermal dosimetry," in *Hyperthermia in Cancer Theraphy*. K. Storm, Ed. Boston, MA: G. K. Hall, 1983, pp. 257-278.

[3] R. B. Roemer, "Ultrasound phantom/animal experiments," in *Physics and Technology of Hyperthermia*, S. B. Field and C. Franconi, Ed. Dordrecht: Nijoff, 1987, pp. 403-413.

[4] P. P. Lele and K. J. Parker, "Temperature distributions in tissue during local hyperthermia by stationary or steered beams of unfocussed or focussed ultrasound, *Brit. J. Cancer*, vol. 45, suppl. V. pp. 108-121, 1982.

[5] K. Hynynen, D. J. Watmough, and J. R. Mallard, "The construction and assessment of lenses for local treatment of malignant tumors by ultrasound," *Ultrasound Med. Biol.*, vol. 9, pp. 33-38, 1983.

[6] P. D. Edmonds, W. C. Ross, E. R. Lee, and P. Fessenden, "Spatial distrubutions of heating by ultrasound transducers in clinical use, indicated in a tissue-equivalent phantom," in *Proc. IEEE Ultrasonic Symp.*, 1985, pp. 908-912.

[7] J. W. Baish, K. R. Foster, and P. S. Ayyaswamy, "Perfused phantom models of microwave irradiated tissue," *ASME J. Biomech Eng.*, vol. 108, pp. 239- 245.

[8] W. L. Lin, R. Roemer, and K. Hynynen, "Theoretical and experimental evaluation of a temperature controller for scanned, focussed ultrasound hyperthermia," *Med. Phys.*, to be published.

[9] P. J. Benkesser, L. A. Frizzell, K. R. Holmes, W. Ryan, C. A. Cain, and S. A. Goss, "Heating of a perfused tissue phantom using a multielement ultrasonic hyperthermia applicator," in *Proc. IEEE Ultrason. Symp.*, 1984. pp. 685-688.

[10] S. Clegg, and R. Roemer, "Towards the estimation of three-dimensional temperature fields from noisy temperature measurements during hyperthermia," *Int. J. Hyper.*, vol. 5, pp. 467-484, 1989.

[11] R. B. Roemer, J. R. Oleson, and T. C. Cetas, "Oscillatory temperature response to constant power applied to canine muscle," *Amer. J. Physiol.*, vol. 249, pp. R153-158, 1985.

[12] P. D. Edmonds, W. C. Ross, E. R. Lee, and P. Fessenden, "SAR profiles of ultrasound transducers in clinical use, indicated by a tissue-equivalent phantom," in *Proc. 34th Ann. Meeting Rad. Res. Soc.*, Las Vegas, NV, 1986. Apr. 12-17, p. 45.

[13] K. R. Holmes, W. Ryan, P. Weinstein, and M. M. Chen, "A fixation technique for organs to be used as perfused tissue phantoms in bioheat transfer studies," *Adv. Bioeng.* R. L. Spilker, Ed., NY: ASME, pp. 9-10.

[14] C. K. Charny, J. L. Guerquin-Kern, M. J. Hagmann, S. W. Levin, and E. E. Lack, W. F. Sindelar, A. Zabell, and E. Glalstein, "Human leg heating using a mini-annular phased array," *Med. Phys.*, vol. 13, pp. 449-456, 1986.

[15] J. B. Zaerr, "Development and evaluation of a dynamic phantom using four independently perfused *in vitro* kidneys as a tool for investigating hyperthermia systems," M.S. Thesis, Univ. Arizona, 1989.

[16] K. Hynynen, R. B. Roemer, D. Anhalt, C. Johnson, Z. X. Zu, W. Swindell, and T. C. Cetas, "A scanned focussed multiple transducer ultrasonic system for localized hyperthermia treatments," *Int. J. Hyperthemia*, vol. 3, p. 21, 1987.

[17] K. Hynynen, D. DeYoung, M. Kundrat, and E. Moros, "The effect of blood perfusion rate on the temperature distributions induced by multiple, scanned and focussed ultrasonic beams in dogs' kidneys *in vivo*," *Int. J. Hyperthermia*, vol. 5, pp. 485-497, 1989.

[18] C. W. Song, "Effect of local hyperthermia on blood flow and microenvironment: A review," *Cancer Res.*, vol. 44, pp. 4721s-4730s, 1984.

[19] A. W. Guy, J. F. Lehmann, and J. B. Stonebridge, "Therapeutic applications of electromagnetic power," *Proc. IEEE*, vol. 62, pp. 55-75, 1974.

[20] H. Tharp, J. Zaerr, and R. Roemer, "Oscillatory temperature response of *in vitro* kidneys induced by temperature controlled flow rates," to be published.

Electrical Stimulation with Pt Electrodes. VIII. Electrochemically Safe Charge Injection Limits with 0.2 ms Pulses

T. L. ROSE AND L. S. ROBBLEE

***Abstract*—The charge injection limits of a Pt electrode using 0.2 ms charge balanced, biphasic current pulses ranged from 50 to 150 $\mu C/cm^2$ geometric if the potential excursions of the electrode are kept below those at which H_2 or O_2 is produced. These charge densities are three to ten times smaller than the currently accepted value based on earlier**

Manuscript received May 4, 1989; revised December 29, 1989. This work was supported by the National Institutes of Neurological and Communicative Disorders and Stroke, National Institutes of Health, under Contracts NO1-NS-4-2363, NO1-NS-5-2379, and NO1-NS-8-2313.

The authors are with Research Division, EIC Laboratories, Norwood, MA 02062.

IEEE Log Number 9038595.

experiments in which the reversible surface reactions were fully utilized and the pulse widths were longer.

Introduction

Platinum remains one of the most commonly used materials for neuronal stimulation [1], [2]. As stimulation electrodes become smaller for more selective excitation, even small currents can result in very high charge densities. Many investigators continue to quote electrochemically safe values of 300–350 $\mu C/cm^2$ real surface area of Pt electrodes [3] which correspond to 420–490 $\mu C/cm^2$ geometric for Pt beads with surface roughness factors of 1.4 [4]. The values were determined with pulse durations longer than 0.6 ms and were based on utilization of all the reversible surface reactions of Pt during a single pulse. For stimulation with shorter pulses and with interpulse potentials near the middle of the potential window between H_2 and O_2 evolution, the charge available from reversible processes is expected to be smaller [5]. As part of our study of new materials for high charge density stimulation, we have reinvestigated Pt under a standard set of conditions [5]–[7]. We report here charge injection values for Pt with biphasic pulses of 0.2 ms/phase using the potentials for hydrogen and oxygen formation as the electrochemically safe potential limits. The values ranged from 50–150 $\mu C/cm^2$ geom, significantly lower than those reported previously.

Experimental

Several types of Pt electrodes were used for these experiments. Type A is a smooth disk, 1.1 mm diam, cut from Pt foil and mounted in a silicone rubber support. Type B is the same as Type A but with the surface roughened by "blasting" it with a high pressure air stream containing 27 μm particles of $NaHCO_3$. The Type A and B electrodes which are the same as those used for a cortical surface array [8], [9] have a geometric area of 9.5×10^{-3} cm^2. Each was cleaned electrochemically by potential cycling in 0.1 M H_2SO_4 prior to pulse testing. The approximate real surface areas determined from the hydride plating reaction [10] was 0.03 cm^2 for Type A (roughness = 3 ×) and 0.05 cm^2 (roughness = 5 ×) for Type B. Type C has a disk geometry made by sealing 0.127 mm diam Pt wire in soft glass and polishing the wire with successively finer alumina grit (to 0.3 μm particle size) until the end of the wire is flush with the glass. The geometric area of the Type C electrode is 1.3×10^{-4} cm^2; its real surface area determined from the hydride plating charge is the same as the geometric area. Type D is a 0.18 mm length of 0.12 mm diam Pt wire extending through a silicone septum to give an exposed geometric surface area of 7.9×10^{-4} cm^2. No roughness factor was measured for this electrode.

The electrochemical measurements were done in a three electrode cell using a 6 cm^2 Pt foil counter electrode oriented parallel to Type A and B electodes, or a large area Pt mesh counter electrode with Type C and D electrodes. A saturated calomel reference electrode (SCE) completed the three-electrode cell. Two electrolytes were used. The Type A and B electrodes were tested in phosphate buffered saline (PBS) (0.02 M or 0.1 M NaH_2Po_4/Na_2HPO_4, 0.12 M NaCl) with 0.02% protein, and Type C and D electrodes in bicarbonate buffered saline (CBS) (0.023 M $NaHCO_3$, 0.1 M NaCl, 5% CO_2 in N_2). The pH of each electrolyte was 7.3. The potential limits chosen for determining the maximum charge that could be injected per pulse were the limits of the potential window for H_2 and O_2 formation as determined by cyclic voltammetry. These limits were −0.60 and +0.90 V versus SCE, respectively.

The biphasic current pulses were charge balanced, capacitively-coupled with either cathodic-first (CF) or anodic-first (AF) polarity. The pulse width was 0.2 ms, and the repetition rate was 50 pps. During the 15 min stimulation period, the potential excursions versus the SCE were monitored on a Tektronix oscilloscope equipped with a 7D20 waveform digitizer. Waveform data were transferred via a GPIB IEEE interface to an IBM-AT for analysis and graphical display. The digitized waveforms had a temporal resolution of 0.9 μs permitting accurate measurement of the access voltage due to the iR drop in the electrolyte (Fig. 1). Potential transients generally reached equilibrium within the first few seconds of pulsing. Fig. 1 shows representative potential transients for one of the electrodes after 15 min of pulsing.

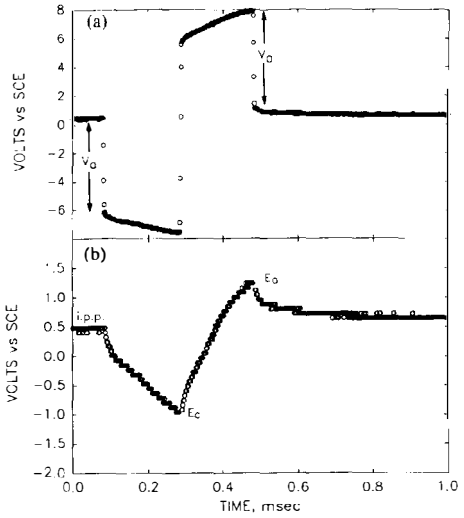

Fig. 1. Potential transient of Type A Pt electrode after 15 min of pulsing in PBS with 400 $\mu C/cm^{-2}$ geom CF biphasic, constant current, 0.2 ms pulses at 50 pps. (a) Original oscilloscope data showing the access voltage (V_a) due to the iR drop in the electrolyte (arrows). (b) Same waveform plotted on expanded scale after correction for iR by subtracting V_a. ipp = interpulse potential; E_c = maximum cathodic potential; E_a = maximum anodic potential.

Results and Discussion

The maximum cathodic and anodic potentials versus SCE, corrected for the access voltage, are plotted as a function of *geometric* charge density in Fig. 2 for AF and CF biphasic pulses. Each data point represents the result of a single 15 min pulse experiment on a given electrode. The solid lines on each graph are the regression curves computed for all the data points shown. The broken lines indicate the operational potential window determined by cyclic voltammetry within which neither H_2 nor O_2 occurs. The reversible charge injection limit is defined as the maximum charge density that can be applied without the electrode potential during pulsing exceeding these potential limits.

Fig. 2 shows that the charge injection limit for anodic-first pulses is about 50–100 $\mu C/cm^2$ geom, and the charge injection limit for cathodic-first pulses is about 100–150 $\mu C/cm^2$. Higher charge densities result in electrode potentials beyond the safe potential window. Considering the differences in electrode size and geometry, there is good agreement between the results of different experiments. The Type C electrode exceeded the cathodic operational limit at a lower charge density than the other electrodes, which may be related to its smaller size and lower roughness.

These charge injection limits are considerably lower than those based on the sum of the charge available from the chemically reversible processes of double-layer charging, H-atom plating and oxidation, and oxidation and reduction reactions of the platinum surface [3]. One explanation for the lower charge injection limits in the present study is that pulsing begins with the electrode potential at an intermediate value between the H_2 and O_2 formation limits. Therefore, all of the reversible processes are not accessible during the leading pulse. The oxide formation and reduction reactions do not occur in the CF pulsing, and the hydride reactions do not occur during AF pulsing. One way to utilize both reactions is to impose an anodic bias on the electrode between pulses. When

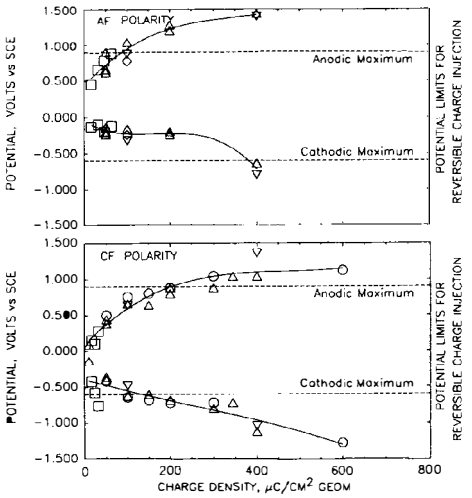

Fig. 2. Potential excursions of Pt electrodes tested with charge balanced, capacitively coupled, biphasic current pulses with AF and CF polarity. The pulse width was 0.2 ms, and the repetition rate was 50 pps. △ = Type A; ▽ = Type A in 0.02 M phosphate buffer; ○ = Type B; □ = Type C; ◇ = Type D; broken lines define the potential window for reversible charge injection.

the type C electrode was biased at 0.9 V verses SCE, up to 600 $\mu C/cm^2$ geom could be injected with 0.2 ms cathodal pulses at 50 pps without the electrode reaching the cathodic potential of −0.6 V verses SCE [6].

A second explanation for the lower charge injection limits is that the rate of the reactions occurring during pulsing may be too slow for them to reach completion, e.g., attain a full monolayer of O or H, during the short 0.2 ms pulse. Longer pulses which permit the reactions to go to completion should result in higher charge limits. Consistent with this hypothesis, Type A electrodes injected 250 $\mu C/cm^2$ with CF pulses and 225 $\mu C/cm^2$ with AF pulses when the pulse duration was increased to 1 ms [11].

Several qualifying comments should be made about the results reported here:

1) The values are normalized to the geometric area of the electrodes. Since most electrodes have some surface roughness making their real surface area larger than their geometric area, the charge injection limits will be lower when normalized to the real surface area.

2) The values reported here are updated guidelines for estimating whether a given charge injected with 0.2 ms biphasic pulses will exceed the reversible charge injection limit. The electrode shape and size has some effect on the potential resulting from a given charge injection as evidenced by the spread in the data shown in Fig. 2. The only certain way to determine a particular electrode's reversible charge injection limit is by measurement of its potential excursions.

3) Other stimulation waveforms may give different charge injection limits. The critical parameters appear to be charge balance, pulse polarity and symmetry, and pulse repetition rate if charge balance is not well maintained. The importance of each of these variables is under current investigation in our laboratory.

4) The potential limits we have defined are conservative, even from an electrochemical standpoint [5], [7], and are well below the levels at which gas bubbles have been observed [12]. Keeping the electrode potential within these limits will guarantee the absence of water electrolysis reactions.

5) We have shown previously that some Pt dissolution occurs even at charge densities of 20–50 $\mu C/cm^2$ geom [9], [13]. During chronic stimulation this dissolution could lead to erosion of the electrode and/or poisoning of the surrounding tissue.

Acknowledgment

The authors wish to thank E. M. Kelliher, A. G. Kimball and X. Beebe for help with experiments conducted in connection with this work.

References

[1] S. B. Brummer, L. S. Robblee, and F. T. Hambrecht, "Criteria for selecting electrodes for electrical stimulation: Theoretical and practical applications," *Ann. NY Acad. Sci.*, vol. 405, pp. 159–171, 1983.

[2] P. E. K. Donaldson, "The role of platinum metal in neurological prosthesis," *Platinum Metals Rev.*, vol. 31, pp. 2–7, 1987.

[3] S. B. Brummer and M. J. Turner, "Electrical stimulation with Pt electrodes. II. Estimation of maximum surface redox (theoretical non-gassing) limits," *IEEE Trans. Biomed. Eng.*, vol. BME-24, pp. 440–443, 1977.

[4] ——, "Electrochemical considerations for safe electrical stimulation of the nervous system with platinum electrodes," *IEEE Trans. Biomed. Eng.*, vol. BME-24, pp. 59–63, 1977

[5] L. S. Robblee and Timothy L. Rose, "Electrochemical guidelines for selection of protocols and electrode materials for neural stimulation," in *Neural Prosthesis: Fundamental Studies*. W. F. Agnew and D. B. McCreery, Eds. Englewood Cliffs, NJ: Prentice-Hall, 1989, pp. 25–66.

[6] E. M. Kelliher and T. L. Rose, "Evaluation of charge injection properties of thin film redox materials for use as neural stimulation electrodes," *Mat. Res. Soc. Symp. Proc.*, vol. 110, pp. 23–27, 1989.

[7] X. Beebe and T. L. Rose, "Charge injection limits of activated iridium oxide electrodes with 0.2 ms pulses in bicarbonate buffered saline," *IEEE Trans. Biomed. Eng.*, vol. BME-35, pp. 494–495, 1988.

[8] L. A. Bullara, W. F. Agnew, T. G. H. Yuen, S. Jacques, and R. H. Pudenz, "Evaluation of electrode array material for neural protheses," *Neurosurg.*, vol. 5, pp. 681–686, 1979.

[9] L. S. Robblee, J. McHardy, W. F. Agnew, and L. A. Bullara, "Electrical stimulation with Pt electrodes. VII. Dissolution of Pt electrodes during electrical stimulation of the cat cerebral cortex," *J. Neurosci. Methods.*, vol. 9, pp. 301–308, 1983.

[10] S. B. Brummer and M. J. Turner, "Electrical stimulation with Pt electrodes. I. A method for determination of "real" electrode areas," *IEEE Trans. Biomed. Eng.*, vol. BME-24, pp. 436–439, 1977

[11] L. S. Robblee, S. F. Cogan, B. Aurian-Blajeni, M. M. Boucher, and A. G. Kimball, "Development of neural stimulating electrodes and evaluation of their electrochemical reactions," 12th Quarterly Prog. NINCDS Contract NO1-NS-5-2379, EIC Laboratories, Oct. 1988.

[12] L. S. Robblee, J. L. Lefko, and S. B. Brummer, "Activated iridium: An electrode suitable for reversible charge injection in saline solution," *J. Electrochem. Soc.*, vol. 130, pp. 731–733, 1983.

[13] L. S. Robblee, J. McHardy, J. M. Marston, and S. B. Brummer, "Electrical stimulation with Pt electrodes. V. The effects of protein on Pt dissolution." *Biomaterials*, vol. 1, pp. 135–139, 1980.